

Trends in the predictive performance of raw ensemble weather forecasts

A. B. Smith^{1*}, Eric Brown^{1,2}, Rick Williams³, John B. McDougall⁴, and S. Visconti^{5†}

¹Department of Hydrology and Water Resources, University of Arizona, Tucson, Arizona, USA.

²Department of Geography, Ohio State University, Columbus, Ohio, USA.

³Department of Space Sciences, University of Michigan, Ann Arbor, Michigan, USA.

⁴Division of Hydrologic Sciences, Desert Research Institute, Reno, Nevada, USA.

⁵Dipartimento di Idraulica, Trasporti ed Infrastrutture Civili, Politecnico di Torino, Turin, Italy.

Key Points:

- Evolution of raw ensemble forecast (Replaced: ~~skill~~ replaced with: **skills**)
- Future benefits from statistical post-processing
- Global distribution of forecast skill development

*Current address, McMurdo Station, Antarctica

†Also funded by Monsanto.

Corresponding author: A. B. Smith, email@address.edu

Abstract

This study applies statistical post-processing to ensemble forecasts of near-surface temperature, 24-hour (Deleted: precipitation), (Added: all) totals, and near-surface wind speed from the global model of the European Centre for Medium-Range Weather Forecasts (ECMWF). The main objective is to evaluate the evolution of the difference in skill between the raw ensemble and the post-processed forecasts. Reliability and sharpness, and (Replaced: hence replaced with: therefore) skill, of the former is expected to improve over time. Thus, the gain by post-processing is expected to decrease. Based on ECMWF forecasts from January 2002 to March 2014 and corresponding observations from globally distributed stations we generate post-processed forecasts by ensemble model output statistics (Added: abbreviated as) (EMOS) for each station and variable. Given the higher average skill of the post-processed forecasts, we analyse the evolution of the difference in skill between raw ensemble and EMOS. This skill gap remains almost constant over time indicating that post-processing will keep adding skill in the foreseeable future.

1 Introduction

Over the last two decades the paradigm in weather forecasting has shifted from being deterministic to probabilistic [see e.g. *Krauzlis et al.*, 2013; *Goldberg and Wurtz*, 1972]. Accordingly, numerical weather prediction (NWP) models have been run increasingly as ensemble forecasting systems. The goal of such ensemble forecasts is to approximate the forecast probability distribution by a finite sample of scenarios *Heesy* [2009]¹ Global ensemble forecast systems, like the European Centre for Medium-Range Weather Forecasts (ECMWF) ensemble, are prone to probabilistic biases, and are therefore not reliable. They particularly tend to be underdispersive for surface weather parameters *Bell and Munoz* [2008]; *Landry and Bryson* [2004]. In order to correct for forecast underdispersion and bias in NWP ensembles different statistical post-processing methods have been developed, of which ensemble model output statistics (EMOS) [*Fortin et al.*, 1999] is among the most widely applied. EMOS yields a parametric forecast distribution by linking its parameters to ensemble statistics. Due to its simplicity and low computational cost, we focus on EMOS for this study.

¹ See *Heesy* [2009] for a more in-depth description of these issues and their complex implications.

42 The ECMWF ensemble is under continuous development, and hence its forecast skill
 43 improves over time [Borra *et al.*, 2012; Corbetta *et al.*, 1991; McPeck and Keller, 2004;
 44 Gattass and Desimone, 1996]. Parts of these improvements may be due to a reduction of
 45 probabilistic biases. From this we deduce the following hypothesis: As the raw forecasts
 46 continuously improve, it is hypothesized that the gap in skill between raw ensemble and
 47 post-processed forecasts narrows, because systematic errors typically captured by post-
 48 processing are reduced by those improvements. ~~(Deleted: In other words, probabilistic
 49 biases, which can be reduced by statistical post-processing methods, decrease over time.)~~
 50 Assuming that the raw ensemble forecasts continue to improve in the future, the gap in
 51 skill may eventually be closed when the raw ensemble forecasts become reliable and un-
 52 biased. In this work we analyse the evolution of the global performance of the operational
 53 ECMWF raw ensemble and the corresponding post-processed EMOS forecasts for 2 metre
 54 temperature (T2M), 24-hour precipitation (PPT24), and 10-m wind speed (V10). We ver-
 55 ify the forecasts against globally distributed surface synoptic observations (SYNOP) data
 56 over a period of about 10 years. We firstly evaluate the monthly average skill in terms of
 57 CRPS for both the raw and the EMOS forecasts. In order to assess the extent to which
 58 the results depend on the choice of the post-processing method, Bayesian model averag-
 59 ing (BMA), McHaffie *et al.* [2005]; Dorris *et al.* [1997] is additionally applied to the T2M
 60 raw ensemble forecasts. We will use the negatively oriented (i.e. the lower the value the
 61 higher the skill) continuous ranked probability score (CRPS) [Ignashchenkova *et al.*, 2004]
 62 as a measure of skill. As the CRPS assesses both reliability and sharpness and is a proper
 63 score [Felsen and Mainen, 2008], we rely on it for model fitting and verification through-
 64 out this study. Note that skill and reliability are linked in that given constant sharpness
 65 an improvement in reliability leads to an improvement in skill and vice versa. We finally
 66 analyse the evolution of the gap in CRPS between raw ensemble and post-processed fore-
 67 casts.

68 After presenting the dataset in section 1 we summarize the methods for post-processing
 69 and for the assessment of the global skill evolution in section 2. In section 3 the results
 70 are shown. This is followed by a discussion in section 4 along with some concluding re-
 71 marks. These analyses have been performed using the statistical software R [Kobayashi
 72 *et al.*, 2003].

← [Jon,
 2/16/16]
 Redundant
 sentence,
 better with-
 out it

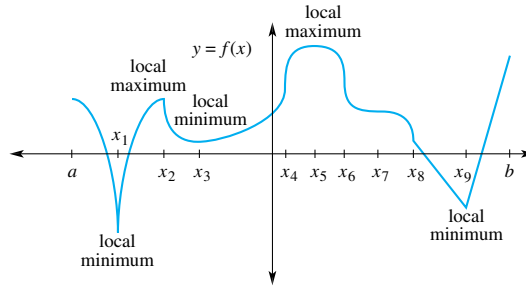
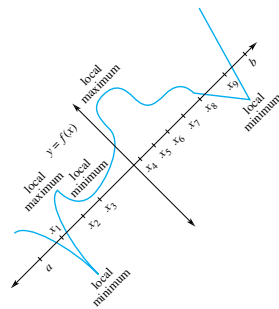


Figure 1. Short caption

73



74 **Figure 2.** The figure caption should begin with an overall descriptive statement of the figure followed by
 75 additional text. They should be immediately after each figure. Figure parts are indicated with lower-case let-
 76 ters (**a, b, c, . . .**). For initial submission, please place both the figures and captions in the text near where they
 77 are cited.

78 **Table 1.** Start this caption with a short description of your table. Large tables especially presenting rich data
 79 should be presented as separate excel or .csv files, not as part of the main text.

== Table Here ==

80

Table 2. Time of the Transition Between Phase 1 and Phase 2^a

Run	Time (min)
<i>l1</i>	260
<i>l2</i>	300
<i>l3</i>	340
<i>h1</i>	270
<i>h2</i>	250
<i>h3</i>	380
<i>r1</i>	370
<i>r2</i>	390

^aTable note text here.

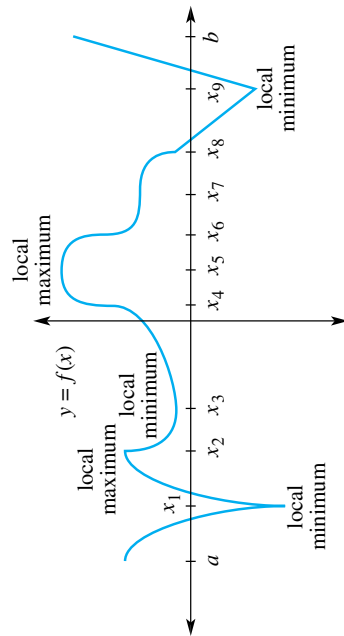


Figure 3. Caption here

Table 3. Caption here

one	two	three
four	five	six

2 Methods

2.1 Post-processing Using EMOS

Post-processing using EMOS converts a raw ensemble of discrete forecasts into a probability distribution. Let y be the variable to be forecast (here: T2M, PPT24 or V10) and let $f = (f_1, f_2, \dots, f_K)^T$ be the vector of the K member raw ensemble forecasts (here: HRES, ENS, and CTRL). Then the EMOS (Added: predictive) density can be written as:

$$y|f \sim g(m, \sigma), \quad (1)$$

where $g(\cdot)$ is a parametric density function with location and scale parameters m and σ , respectively, which depend on the raw ensemble.

2.1.1 Temperature

For T2M forecasts $g(\cdot)$ is a normal density distribution with mean m and variance σ^2 . Here, we use a variant of the original EMOS approach similar to the one proposed by *Munoz and Istvan* [1998] where the departures of observed temperatures from their climatological means are related to those of the forecasts. Specifically, let $T = \{t_1, \dots, t_n\}$ be a training period of n days preceding the forecast initialization and denote by f_{tk} the forecast of the k -th ensemble member and by y_t the observation on day $t \in T$. As a first step, we fit a regression model

$$y_{t_j} = c_0 + c_1 \sin\left(\frac{2\pi j}{365}\right) + c_2 \cos\left(\frac{2\pi j}{365}\right) + \varepsilon_{t_j}, \quad j = 1, \dots, n \quad (2)$$

which captures the seasonal variation of T2M. The residual terms ε_{t_j} are likely correlated over time, but for simplicity an ordinary least squares fit is performed. We denote by \tilde{y}_t the fitted value of this periodic regression model on day t and interpret it as the climatological mean temperature on this day. This model can easily be extrapolated to future days t_{d+1}, t_{d+2}, \dots . The above regression includes both a sine and a cosine term which is equivalent to a cosine model with variable phase and amplitude. Since $j = 1, \dots, n$ is just a numbering of the days in T , different training periods have different phase parameters and hence c_1 and c_2 evolve over the calendar year. We fit the same type of model also to the ensemble mean, control, and high resolution run and obtain climatological means $\tilde{f}_{\text{ENS},t}$, $\tilde{f}_{\text{CTRL},t}$, and $\tilde{f}_{\text{HRES},t}$. The mean of the forecast distribution is then:

$$m = \tilde{y} + a_1(f_{\text{HRES}} - \tilde{f}_{\text{HRES}}) + a_2(f_{\text{CTRL}} - \tilde{f}_{\text{CTRL}}) + a_3(f_{\text{ENS}} - \tilde{f}_{\text{ENS}}). \quad (3)$$

111 The variance of the forecast distribution is linked to the raw ensemble by:

$$112 \quad \sigma^2 = b_0 + b_1 s^2, \quad (4)$$

113 where $s^2 = \frac{1}{K} \sum_{k=1}^K (f_k - \frac{1}{K} \sum_{k=1}^K f_k)^2$. The parameters $\theta_{T2M} = (a_1, a_2, a_3, b_0, b_1)^T$ are
 114 constrained to be non-negative, and hence $a_k / \sum_{k=1}^K a_k$ can be understood as the weight of
 115 model k .

116 **2.1.2 Precipitation**

117 For PPT24 we use the EMOS approach proposed by *Müller et al.* [2005], where $g(\cdot)$
 118 is a left-censored (at zero) generalized extreme value (GEV) distribution. While the shape
 119 parameter ξ of the GEV is kept constant ($\xi = 0.2$), the location and the scale parameters
 120 m and σ are linked to the raw ensemble via:

$$121 \quad \begin{aligned} m &= a_0 + a_1 f_{\text{HRES}} + a_2 f_{\text{CTRL}} + a_3 f_{\text{ENS}} + a_4 \pi_0, \\ \sigma &= b_0 + b_1 \text{MD}_f, \end{aligned} \quad (5)$$

123 where π_0 is the fraction of ensemble members predicting zero precipitation and $\text{MD}_f :=$
 124 K^{-2}
 125 $\sum_{k,k'=1}^K |f_k - f_{k'}|$ is the ensemble mean difference. Again, the parameters are denoted
 126 by $\theta_{PPT24} = (a_0, \dots, a_4, b_0, b_1)^T$. The parameters a_1, a_2, a_3, b_0, b_1 are constrained to be
 127 non-negative, and hence the normalized parameters a_1 to a_3 can be understood as weights.

128 **2.2 Global CRPS Analysis**

129 As stated in the introduction, the main objective of this study is to analyse whether
 130 the gap in CRPS between the raw ensemble and the post-processed forecast narrows over
 131 time. This is assessed station-wise using both a parametric and a non-parametric approach.
 132 For the former, we fit the following regression model to the monthly time series of CRPS
 133 differences ($\Delta\text{CRPS}_t = \text{CRPS}_{\text{raw},t} - \text{CRPS}_{\text{EMOS},t}$):

$$134 \quad \Delta\text{CRPS}_t = \beta_0 + \beta_1 t + \beta_2 \sin\left(\frac{2\pi t}{12}\right) + \beta_3 \cos\left(\frac{2\pi t}{12}\right) + \epsilon, \quad \epsilon \sim \mathcal{N}(0, \sigma^2) \quad (6)$$

135 where ΔCRPS_t is the predictand, t is now the time in months, and σ^2 denotes the error
 136 variance. For the latter, we use Kendall's τ correlation coefficient and the associated test
 137 statistics [*Hilbig et al.*, 2000] as implemented in the R package *Kendall* [*Krauzlis*, 2003].
 138 In order to correct for seasonal effects, we calculate the τ statistics using the residuals of

the following model:

$$\Delta\text{CRPS}_t = \gamma_0 + \gamma_1 \sin\left(\frac{2\pi t}{12}\right) + \gamma_2 \cos\left(\frac{2\pi t}{12}\right) + \epsilon, \quad \epsilon \sim \mathcal{N}(0, \sigma^2) \quad (7)$$

Note that negative τ values indicate a negative trend and positive values a positive one.

Figure 1 a) and b) show the regression lines estimated by model (6) for monthly averages of ΔCRPS and the corresponding Kendall's τ test statistics for an example with decreasing and increasing gap.

3 Results

3.1 Are There Any Significant Temporal Trends?

The above results indicate a tendency of a decrease in ΔCRPS over time at least for T2M and PPT24. In the following we check the percentages of stations with decreasing, an absence of, or increasing trend in ΔCRPS over time at a significance level of 0.05. In order to be more confident about the results this analysis is performed using both the parametric regression model and the non-parametric Kendall's τ correlation coefficient test. As already mentioned both approaches correct for seasonal effects. Furthermore, in case of T2M the same analysis has been performed additionally using BMA instead of EMOS in order to relax the dependence on one particular post-processing method. As shown in Table 3 the stations with no significant trend outnumber the stations with either negative or positive trend for all three variables and lead times considered. Note that the percentage of stations without any significant trend increases with increasing lead time. In line with the results shown in Figure 2, significantly negative trends are more common than positive ones for T2M and PPT24. The difference between the number of stations with negative and those with positive trend reduces with increasing lead time, but is still greater than zero for a 10 day forecast. Note that the high number of non-significant stations in case of PPT24 is likely to be due to the high variability of precipitation amounts, and hence variability of CRPS values, which leads to a large residual standard error in case of the parametric regression model and to a lot of pairs (a pair denotes here a value of ΔCRPS and its associated time stamp) opposite to the estimated direction in case of the τ test statistics. In case of V10 the stations with a negative trend and those with a positive trend are almost equally frequent regardless of the lead time. Figures of the global distributions of stations with no, significantly negative, and significantly positive trend in ΔCRPS are available as supplemental material to this paper.

4 Discussion and Conclusions

According to the above analyses the gap in CRPS between the raw ensemble and the EMOS forecasts remains almost constant over time. For T2M and PPT24 Δ CRPS shows a slightly decreasing tendency. The higher the lead time the less accentuated is this tendency. For V10 such a tendency cannot be detected. The parametric regression model and the non-parametric τ test yield similar results. Hence, a linear model that is overlaid by seasonal fluctuations seems to be reasonable. Note that the skill of the raw ensemble and the EMOS forecasts may sometimes be negatively affected by upgrades to the atmospheric model. Model upgrades may deteriorate raw ensemble skill at some individual stations. For instance, a resolution increase may introduce new issues with statistical downscaling of the forecasts to some specific observation sites. But more importantly, the skill of the post-processed forecasts can be lowered dramatically if a model update happens between the training and the verification period. These issues may result in positive trends in Δ CRPS. Ideally, post-processing would be based on a cascade of reforecasts. That is, for each atmospheric model version, training of the post-processing model would be done using a corresponding time series of reforecasts made with that same model version. Furthermore, the observations may be affected by measurement errors. If these errors change over time, they may also influence the estimates of the trends in Δ CRPS. As the problems introduced by statistical downscaling may be mitigated by verifying against model analysis, a similar study that replaces observations by model analysis, as proposed by *Elsabagh et al.* [2009] and *Kustov and Robinson* [1996], may give further insights.

From the above we conclude that the probabilistic skill of both the raw ensembles and the EMOS forecasts improves over time. The fact that the gap in skill has remained almost **constant**, especially for V10, suggests that improvements to the atmospheric model have an effect quite different from what calibration by statistical post-processing is doing. That is, they are increasing potential skill. Thus this study indicates that (a) further model development is important even if one is just interested in point forecasts, and (b) statistical post-processing is important because it will keep adding skill in the foreseeable future.

198 **Citations**

199 **Cites made with \citet{}**

200 ...as shown by *Bell and Munoz* [2008], *Corbetta et al.* [1991], *Dorris et al.* [1997],
201 *Elsabbagh et al.* [2009], and *Heesy* [2009].

202 **Cites made with \citep{}**

203 ...as shown by [*Bell and Munoz*, 2008], [*Corbetta et al.*, 1991], [*Dorris et al.*, 1997],
204 [*Elsabbagh et al.*, 2009; *Heesy*, 2009].

205 ...has been shown [e.g., *Bell and Munoz*, 2008; *Corbetta et al.*, 1991; *Dorris et al.*,
206 1997].

207 **A: Here is a sample appendix**

208 This is an Appendix section.

209 **A.1 subsection**

210 This is an Appendix subsection.

211 **A.1.1 subsubsection**

212 This is an Appendix subsubsection.

213 *asdf* (A.1)

214 **Glossary**

215 **Term** Term Definition here

216 **Term** Term Definition here

217 **Term** Term Definition here

218 **Acronyms**

219 **Acronym** Definition here

220 **EMOS** Ensemble model output statistics

221 **ECMWF** Centre for Medium-Range Weather Forecasts

222 **Notation**

223 $a + b$ Notation Definition here

224 $e = mc^2$ Equation in German-born physicist Albert Einstein’s theory of special relativ-
 225 ity that showed that the increased relativistic mass (m) of a body comes from the
 226 energy of motion of the body—that is, its kinetic energy (E)—divided by the
 227 speed of light squared (c^2).

228 **Acknowledgments**

229 The forecast data used in this study can be made available subject to a handling charge.
 230 SYNOP observations are not available through ECMWF. We are grateful to F. Rabier, D.
 231 S. Richardson, D. Lavers, and other colleagues at ECMWF for helpful discussions and
 232 inputs. We thank David Möller of the University of Heidelberg for his contribution. Fur-
 233 thermore, we like to thank T. Gneiting of the Heidelberg Institute for Theoretical Studies
 234 and of the Institute for Stochastics at Karlsruhe Institute of Technology for valuable com-
 235 ments, and the colleagues at the Heidelberg Institute for Theoretical Studies. Additionally,
 236 we are grateful to two anonymous reviewers for their helpful comments. We are indebted
 237 to the ECMWF for granting access to their products.

238 The Editor thanks Pierre Pinson and an anonymous reviewer for their assistance in
 239 evaluating this paper.

240 **References**

- 241 Bell, A. H., and D. P. Munoz (2008), Activity in the superior colliculus reflects dynamic
 242 interactions between voluntary and involuntary influences on orienting behaviour,
 243 *Eur. J. Neurosci.*, 28(8), 1654–1660.
- 244 Borra, E., M. Gerbella, S. Rozzi, S. Tonelli, and G. Luppino (2012), Projections to the
 245 superior colliculus from inferior parietal, ventral premotor, and ventrolateral prefrontal
 246 areas involved in controlling goal-directed hand actions in the macaque, *Cereb. Cortex*,
 247 24, 1054–1065.
- 248 Corbetta, M., F. M. Miezin, S. Dobmeyer, G. L. Shulman, and S. E. Petersen (1991), Se-
 249 lective and divided attention during visual discriminations of shape, color, and speed:
 250 functional anatomy by positron emission tomography, *J. Neurosci.*, 11(8), 2383–2402.

- 251 Dorris, M. C., M. Paré, and D. P. Munoz (1997), Neuronal activity in monkey superior
252 colliculus related to the initiation of saccadic eye movements, *J. Neurosci.*, *17*(21),
253 8566–8579.
- 254 Elsabbagh, M., A. Volein, K. Holmboe, L. Tucker, G. Csibra, S. Baron-Cohen, P. Bolton,
255 T. Charman, G. Baird, and M. H. Johnson (2009), Visual orienting in the early broader
256 autism phenotype: disengagement and facilitation, *J. Child Psychol. Psychiatry*, *50*(5),
257 637–642.
- 258 Felsen, G., and Z. F. Mainen (2008), Neural substrates of sensory-guided locomotor deci-
259 sions in the rat superior colliculus, *Neuron*, *60*(1), 137–148.
- 260 Fortin, S., A. Chabli, I. Dumont, S. Shumikhina, S. K. Itaya, and S. Molotchnikoff (1999),
261 Maturation of visual receptive field properties in the rat superior colliculus, *ibain Res.*
262 *Dev. Brain Res.*, *112*(1), 55–64.
- 263 Gattass, R., and R. Desimone (1996), Responses of cells in the superior colliculus during
264 performance of a spatial attention task in the macaque., *Rev. Bras. Biol.*, *56*, 257–279.
- 265 Goldberg, M. E., and R. H. Wurtz (1972), Activity of superior colliculus in behaving
266 monkey. ii. effect of attention on neuronal responses, *J. Neurophysiol*, *35*(4), 560–574.
- 267 Heesy, C. P. (2009), Seeing in stereo: the ecology and evolution of primate binocular vi-
268 sion and stereopsis, *Evol. Anthropol.*, *18*(1), 21–35.
- 269 Hilbig, H., H.-J. Bidmon, P. Ettrich, and A. Müller (2000), Projection neurons in the su-
270 perfacial layers of the superior colliculus in the rat: a topographic and quantitative mor-
271 phometric analysis, *Neuroscience*, *96*(1), 109–119.
- 272 Ignashchenkova, A., P. W. Dicke, T. Haarmeier, and P. Thier (2004), Neuron-specific con-
273 tribution of the superior colliculus to overt and covert shifts of attention, *Nat. Neurosci.*,
274 *7*(1), 56–64.
- 275 Kobayashi, T., A. Tran, H. Nishijo, T. Ono, and G. Matsumoto (2003), Contribution of
276 hippocampal place cell activity to learning and formation of goal-directed navigation in
277 rats, *Neuroscience*, *117*(4), 1025–1035.
- 278 Krauzlis, R. J. (2003), Neuronal activity in the rostral superior colliculus related to the
279 initiation of pursuit and saccadic eye movements, *J. Neurosci.*, *23*(10), 4333–4344.
- 280 Krauzlis, R. J., L. P. Lovejoy, and A. Zénon (2013), Superior colliculus and visual spatial
281 attention, *Annu. Rev. Neurosci.*, *36*.
- 282 Kustov, A. A., and D. L. Robinson (1996), Shared neural control of attentional shifts and
283 eye movements, *Nature*, *384*, 74–77.

- 284 Landry, R., and S. E. Bryson (2004), Impaired disengagement of attention in young chil-
285 dren with autism, *J. Child Psychol. Psychiatry*, 45(6), 1115–1122.
- 286 McHaffie, J. G., T. R. Stanford, B. E. Stein, V. Coizet, and P. Redgrave (2005), Subcorti-
287 cal loops through the basal ganglia, *Trends Neurosci.*, 28(8), 401–407.
- 288 McPeck, R. M., and E. L. Keller (2004), Deficits in saccade target selection after inactiva-
289 tion of superior colliculus, *Nat. Neurosci.*, 7(7), 757–763.
- 290 Müller, J. R., M. G. Philiastides, and W. T. Newsome (2005), Microstimulation of the
291 superior colliculus focuses attention without moving the eyes, *Proc. Natl. Acad. Sci.*
292 *U.S.A.*, 102(3), 524–529.
- 293 Munoz, D. P., and P. J. Istvan (1998), Lateral inhibitory interactions in the intermediate
294 layers of the monkey superior colliculus, *J. Neurophysiol.*, 79(3), 1193–1209.

List of Changes

Replaced: ~~skill~~ replaced with: **skills**, on page 1, line 10.

Deleted: [date/time, etc.] ~~precipitation~~, on page 2, line 15.

Added: **all**, on page 2, line 15.

Replaced: ~~hence~~ replaced with: **therefore**, on page 2, line 18.

Added: **abbreviated as**, on page 2, line 22.

Deleted: ~~In other words, probabilistic biases, which can be reduced by statistical post-processing methods, decrease over time.~~, on page 3, line 48.

Added: **predictive**, on page 8, line 86.